

ir absorption of CN^- defects in cesium halides rotationally aligned by alkali-metal-ion impurities

Wolf von der Osten* and Fritz Lüty

Physics Department, University of Utah, Salt Lake City, Utah 84112

(Received 3 November 1986)

Substitutional CN^- defects in CsCl, CsBr, and CsI show under increasing temperature strong broadening of their ir stretching absorption line ν_0 into unresolved vibrational-rotational spectra characteristic of a quasifree rotor. Additional K^+ or Rb^+ impurities in these hosts produce two extra CN^- absorption lines ν_1 and ν_2 (at lower energy than ν_0), which remain sharp and resolved to high temperatures. These two lines, which we studied in the fundamental and second-harmonic absorption spectra as a function of temperature, are caused by a CN^- -alkali-ion impurity complex. While the CN^- elastic dipole is rotationally aligned along the axis of the complex, its electric dipole can have two opposite orientations thus producing the two vibrational absorption lines ν_1 and ν_2 . Tentative models for the reorientation between the two localized CN^- configurations are discussed.

I. INTRODUCTION

CN^- molecular ions, substituted in dilute (noninteracting) form into alkali halide crystals, represent model systems for elastic and electric dipole defects in ionic crystals. Extended studies of their elasto- and electro-optical properties^{1,2} as well as Raman spectroscopy³ established their dipole orientations in the cubic lattice, which in potassium and rubidium halides are the eight equivalent $\langle 111 \rangle$ directions. The defect-lattice interaction potential, which hinders the CN^- reorientational motion, is, however, very weak in these hosts. Early work by Narayanamurti and Pohl showed that the sharp CN^- stretching-mode absorption (at $\sim 4.8 \mu\text{m}$) broadens drastically with increasing temperature into an unresolved vibrational-rotational spectrum of a quasifree rotor.⁴ The weak energy barriers of the rotation-hindering potential produce sizable tunneling splitting of the orientational states, as observed by high-resolution ir (Ref. 1) and Raman (Ref. 3) spectroscopy of the CN^- stretching mode. For cesium halide hosts, treated in this work, neither equilibrium orientations nor tunneling splitting of CN^- defects have been established by any experiment. The strong temperature broadening of the CN^- stretching-mode absorption, however, indicates quasifree rotation in a weak hindering potential comparable to that in the above-mentioned hosts.

A strongly revived interest in CN^- systems originates from the recent discovery of vibrational ($\sim 4.8 \mu\text{m}$) fluorescence, emitted by vibrationally excited CN^- defects in alkali halides.⁵ The required excitation was produced either by electron-vibrational ($e-v$) coupling of the CN^- defect to a neighboring optically excited F center⁵, or by direct ir excitation of CN^- defects in their overtone vibrational absorption band, using tunable color-center lasers.⁶ Both these techniques revealed the following CN^- vibrational emission properties in cesium halide hosts: by far the most efficient $e-v$ coupling for excitation, producing superfluorescence and laser operation,⁷ and the longest vibrational lifetime extended to high tem-

peratures.⁸ Besides these properties, direct ir second-harmonic pumping of the CN^- fluorescence in CsCl revealed the existence of two sharp excitation peaks, spectrally located close to the absorption line of the isolated CN^- defect.⁸

Because of the promising vibrational emission and laser properties of CN^- defects in cesium halides, we systematically explore in this work the existence, nature, and physical origin of the CN^- sharp-line absorption in these hosts. This investigation led to the discovery of defect complexes formed by the association of alkali-ion impurities (K^+ and Rb^+) with CN^- defects in CsCl, CsBr, and CsI, which are characterized by the fundamental and second-harmonic CN^- stretching absorption. Parallel to the work on cesium halides presented here, we have observed and studied various defect-associated CN^- molecules in alkali halides of NaCl structure. First results—particularly on CN^- in KCl and KBr doped with Rb^+ , Na^+ , and Li^+ impurities—have been reported previously^{8,9} and will be published in detail separately. Spitzer *et al.*¹⁰ have recently studied the Na^+ -associated CN^- defect in KBr, and achieved interesting spectral hole burning in its sharp fundamental absorption.

II. EXPERIMENTAL TECHNIQUES AND RESULTS

The single- or double-doped cesium halide crystals were grown by the Czochralski technique in the Utah Crystal Laboratory. CsCN as doping material produces CN^- defects only, while KCN or RbCN dopants produce a fixed (close to 1:1) ratio of alkali-metal ion and CN^- impurities in the host. In order to increase this ratio, potassium or rubidium halides (with the same halogen as the host crystal) can be added as dopant at any desired level [e.g., $\text{CsBr} + x(\text{KCN}) + y(\text{KBr})$]. The actual concentrations in the crystal were determined for the alkali impurities by atomic absorption spectroscopy, and for the CN^- impurities by titration and from the melt-to-solid distribution coefficient. All reported numbers are actual concentra-

tions in the crystal.

From a great variety of crystals, doping concentrations, and absorption measurements in the CN^- fundamental and overtone spectral range at various temperatures, we display in Fig. 1–3 some selected characteristic data. Figure 1 shows for $\text{CsCl}:\text{CN}^-$ doped with an excess of K^+ or Rb^+ impurities the CN^- fundamental between 20 and 240 K. Similar measurements (extending to 8 K) in $\text{CsBr}:\text{CN}^-$ with added K^+ or Rb^+ , and in $\text{CsI}:\text{CN}^-$ with added Rb^+ impurities, are shown in Fig. 2. In all five cases, two narrow absorption lines (ν_1) and (ν_2) of different separation ($\nu_1 - \nu_2$) are observed, located on the low-energy side of the well-known CN^- stretching-mode absorption (ν_0). In order to test the nature and anharmonicity of these new lines ν_1 and ν_2 , and to improve the spectral resolution of the ν_0, ν_1, ν_2 separation, similar absorption measurements were done in the CN^- second-harmonic ($\sim 2.4 \mu\text{m}$) region. In spite of the 100 times weaker overtone absorption strength compared to the fundamental, thicker crystal samples of reasonably high CN^- concentrations allowed accurate measurements. Figure 3 shows as one example second-harmonic CN^- absorption measurements in $\text{CsCl}:\text{CN}^-$ (with added K^+ or Rb^+) and

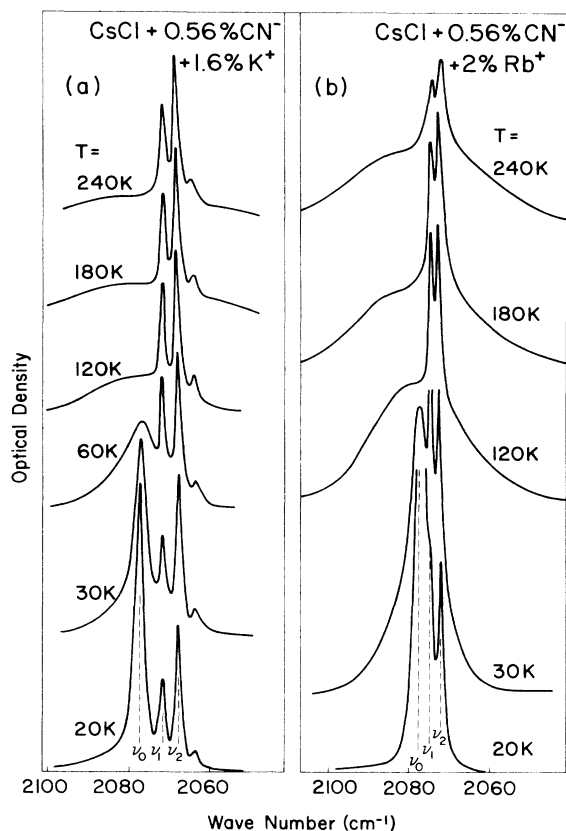


FIG. 1. Fundamental CN^- vibrational absorption spectra between 20 and 240 K of $\text{CsCl} + 0.56 \text{ mol } \% \text{CN}^-$, containing additionally (a) 1.6 mol % K^+ and (b) 2.0 mol % Rb^+ impurities.

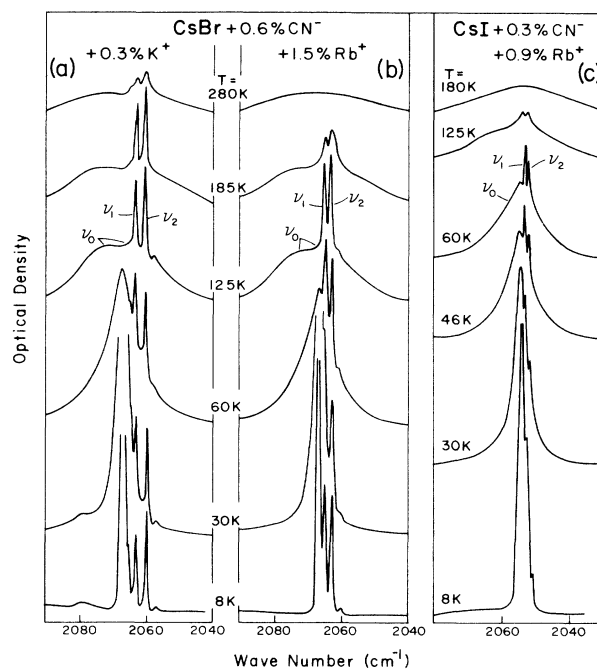


FIG. 2. Fundamental CN^- vibrational absorption spectra measured between 8 K and 280 or 180 K in the following: (a) $\text{CsBr} + 0.6 \text{ mol } \% \text{CN}^- + 0.3 \text{ mol } \% \text{K}^+$; (b) $\text{CsBr} + 0.6 \text{ mol } \% \text{CN}^- + 1.5 \text{ mol } \% \text{Rb}^+$; (c) $\text{CsI} + 0.3 \text{ mol } \% \text{CN}^- + 0.9 \text{ mol } \% \text{Rb}^+$.

in $\text{CsI}:\text{CN}^-$ with K^+ impurities. As in Figs. 1 and 2, the ν_0 , ν_1 , and ν_2 lines appear again in overtone absorption, under improved instrumental resolution and with about doubled spectral separation.

From comparison with cesium halide samples which were doped with CN^- without additional alkali-metal-ion

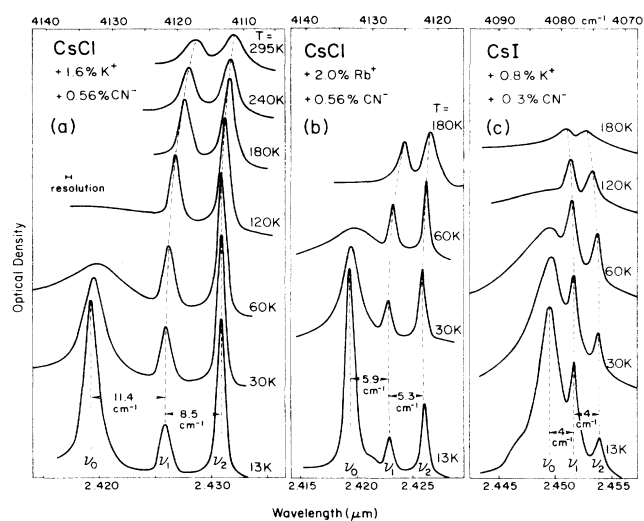


FIG. 3. Second-harmonic CN^- vibrational absorption spectra measured between 13 K and 295 or 180 K in the following: (a) $\text{CsCl} + 0.56 \text{ mol } \% \text{CN}^- + 1.6 \text{ mol } \% \text{K}^+$; (b) $\text{CsCl} + 0.56 \text{ mol } \% \text{CN}^- + 2.0 \text{ mol } \% \text{Rb}^+$; (c) $\text{CsI} + 0.3 \text{ mol } \% \text{CN}^- + 0.8 \text{ mol } \% \text{K}^+$.

TABLE I: Fundamental and second-harmonic stretching frequency ν (in cm^{-1}) of CN^- molecules in CsCl, CsBr, and CsI. ν_0 refers to the ir absorption band (at 15 K) of isolated CN^- defects, ν_1 and ν_2 to the two sharp lines, produced by CN^- associated to either K^+ or Rb^+ impurities.

Host	Impurity	Fundamental (cm^{-1})			Second harmonic (cm^{-1})		
		ν_0	$\nu_0 - \nu_1$	$\nu_0 - \nu_2$	ν_0	$\nu_0 - \nu_1$	$\nu_0 - \nu_2$
CsCl	K^+	2078	6	10	4134	11	20
	Rb^+		3	5		6	11
CsBr	K^+	2067	4	7	4110	8	15
	Rb^+		2	4			
CsI	K^+	2054	2	4	4083	4	8
	Rb^+		2	3			

impurities and which exclusively exhibit the unperturbed CN^- vibrational absorption (ν_0), we attribute the new lines to vibrational transitions of CN^- -impurity complexes formed. This assumption is supported by the temperature dependence of these lines also illustrated in the figures. While isolated CN^- defects—due to their quasi-free rotational behavior—show strong temperature broadening of their stretching-mode vibrational absorption, the vibrational absorptions of CN^- -impurity complexes preserve their narrow linewidth up to high temperatures. This indicates orientational alignment of the CN^- defect by the associated impurity. As expected from this model, the integrated absorption strength of the $\nu_1 + \nu_2$ lines relative to the free- CN^- ν_0 absorption increases about linearly with the alkali-ion- CN^- concentration ratio.

In addition to the absorption spectra described above, which are due to the main isotope $^{12}\text{C}^{14}\text{N}$ (relative abundance 98.5%), we were able in an extremely thick sample to also observe the sharp lines ν_1 and ν_2 accompanying the fundamental stretching vibration ν_0 of the $^{13}\text{C}^{14}\text{N}$ isotope. According to its small relative abundance ($\sim 1.1\%$), these transitions are considerably weaker. The ratio of integrated absorptions of the unperturbed and rotationally localized CN^- vibrations, however, is roughly equal for the two isotopes. This further supports our interpretation, in particular ruling out any effect of localization due to CN^- pairs that might be expected at higher CN^- concentrations.

From the material presented in Figs. 1–3 and in Table I several systematic trends can be noticed for the ν_1 and ν_2 absorption lines due to the CN^- -impurity complex.

(1) Both the *energy shifts* from the unperturbed stretching mode ν_0 and the *energy splitting* of the two lines $\Delta\nu = \nu_1 - \nu_2$ decrease monotonically along the host lattice series $\text{CsCl} \rightarrow \text{CsBr} \rightarrow \text{CsI}$, and in each host with $\text{K}^+ \rightarrow \text{Rb}^+$ impurity variation. Particularly in CsI, for which the shifts and splittings are the smallest, ν_1 and ν_2 give rise merely to weak shoulders on the low-energy part of the narrow ν_0 absorption line [Fig. 2(c)]. They can, however, be better resolved at intermediate temperatures (~ 40 – 100 K) when they are located as still reasonably sharp lines on top of a strongly broadened ν_0 band background. Clearly again, the overtone measurements with

energy shift and splitting values doubled are superior for spectral resolution and reveal more details. Figure 3 shows (indicated by a dashed line) that the ν_1 and ν_2 lines shift with increasing temperature—for CsCl to lower and for CsI to higher energies. Beyond this the line splitting $\nu_1 - \nu_2$ reduces lightly with increasing temperature. As this reduction of splitting occurs essentially in the temperature range of line broadening, it could be caused—at least partially—by increasing spectral overlap of the two broadening bands.

(2) The *widths of the new absorption lines* are small (< 2 cm^{-1}) and may be at the lowest temperatures (8 or 13 K) below the resolution limit of our instrument. In contrast to the CN^- vibrational absorption line which exhibits the strongly temperature-dependent linewidth, the localized transitions remain narrow up to much higher temperatures. In CsCl thermal broadening of the K^+ - CN^- complex starts at ~ 150 K, and even at room temperature the lines are still observable as a relatively narrow and distinct double-peak structure. In CsBr and CsI thermal broadening of the same complex sets in already at lower temperatures, the lines remaining sharp only up to ~ 240 and ~ 180 K, respectively. In these three hosts the ν_1, ν_2 lines of the Rb^+ - CN^- complex broaden and wash out at lower temperature compared to the lines of the K^+ - CN^- complex. This host lattice and impurity trend is the same one as discussed under (1), showing that the temperature of beginning line broadening scales with the size of their energy splitting $\Delta\nu$.

(3) The observed *ratio of integrated absorptions* (I_1/I_2) of the two localized transitions ν_1 and ν_2 shows a systematic trend with crystal matrix size also. While this ratio is clearly < 1 for CsCl, it becomes closer to 1 in CsBr and > 1 in CsI. From Figs. 1–3 this trend is seen to hold for the fundamental as well as the overtone absorption. All measurements illustrated in Figs. 1–3, however, show clearly that the ratio (I_1/I_2) is temperature dependent and approaches in all cases the value of ~ 1 at high temperatures.

III. DISCUSSION

The reported measurements strongly suggest the formation of defect complexes involving CN^- molecules and al-

kali impurities. An approximate linear scaling of the ν_1, ν_2 bands with K⁺ or Rb⁺ concentration (at least at low doping levels) indicates clearly that only *one* alkali-metal-impurity is involved in the complex, and the same evident observation and conclusion is valid for the CN⁻ defect also.

In Fig. 4 we give a schematic illustration of the microscopic structure of the CN⁻ defect and the two complexes which give rise to the three observed $\nu_0, \nu_1,$ and ν_2 vibrational absorptions. Although—in contrast to other alkali-halide crystals—for cesium halides no investigations exist from which the equilibrium orientations of the CN⁻ defect are known, based on the crystal structure it is reasonable to assume a $\langle 111 \rangle$ symmetry [Fig. 4(a)]. In similarity to the CN⁻-doped potassium and rubidium halides, this system behaves like a weakly hindered rotor. At low temperature, the internal molecular stretching vibration gives rise to the narrow absorption line ν_0 . At higher temperatures, thermal excitation of vibrational-rotational states leads to the well-known broadening and change in line shape.

The simplest model of a perturbed CN⁻ defect that qualitatively would explain our results presented above is illustrated in Fig. 4(b). Here we assume one of the cesium ions in the first shell around the CN⁻ defect (substituted onto an anion site) to be replaced by the alkali impurity. If we first disregard the head and tail difference and the electric dipole moment of the CN⁻ we expect that the lowering of symmetry ($O_h \rightarrow C_{3v}$) of the CN⁻ rotation potential due to the alkali impurity will have a strong effect on the CN⁻ orientation. As the CN⁻ molecule is a “cigar-shaped” elastic dipole (elongated along its axis), the reduction of repulsive interaction by the introduction of a small size neighbor will produce considerably lower energy for alignment of the CN⁻ molecule along the axis of the defect pair. It is further well known, from host ma-

terial variation, pressure experiments, and model calculations¹¹ that the frequency of the CN⁻ stretching mode depends strongly on repulsive interaction, shifting to higher energies with decreasing lattice spacing. In our case, the exchange of one large Cs⁺ ion by a smaller Rb⁺ or K⁺ ion will increase the spacing along the defect pair axis. This predicts a general shift of the CN⁻ stretch mode to lower energies, but a smaller shift for Rb⁺ compared to K⁺—exactly as observed in all three hosts. Furthermore, the gain of space by K⁺ or Rb⁺ substitution relative to the space available in the pure lattice will increase from CsI \rightarrow CsBr \rightarrow CsCl. We therefore expect a parallel increase in the shift of the perturbed CN⁻ stretching mode with this host material variation. This again is in full agreement with the experimental results.

The heteronuclear structure of the CN⁻ and the different cation neighbors along the $\langle 111 \rangle$ axis of the aligned CN⁻ elastic dipole removes the inversion symmetry, creating two different configurations I and II of opposite orientation for the CN⁻ molecule, as illustrated in Fig. 4(b). As the carbon end is known to be slightly less negative than the nitrogen end, CN⁻ carries a small ($p \approx 0.3$ D) electric dipole, indicated by an arrow in Fig. 4. The repulsive and electrostatic interaction of the C and N molecular ends with the two different Cs⁺ and (K⁺ or Rb⁺) neighbors along the $\langle 111 \rangle$ axis can produce different energies for the two opposite states. Moreover, they can produce two different center-of-mass displacements of the CN⁻ along the axis, creating by this off-center shifts different effective electric dipole moments in the two opposite states.

The observed splitting of the low-energy shifted CN⁻ stretching mode into a doublet (ν_1, ν_2) is in good qualitative agreement with these considerations. If the energy of the two opposite orientations would happen to be about the same and a sizable tunneling matrix element would ex-

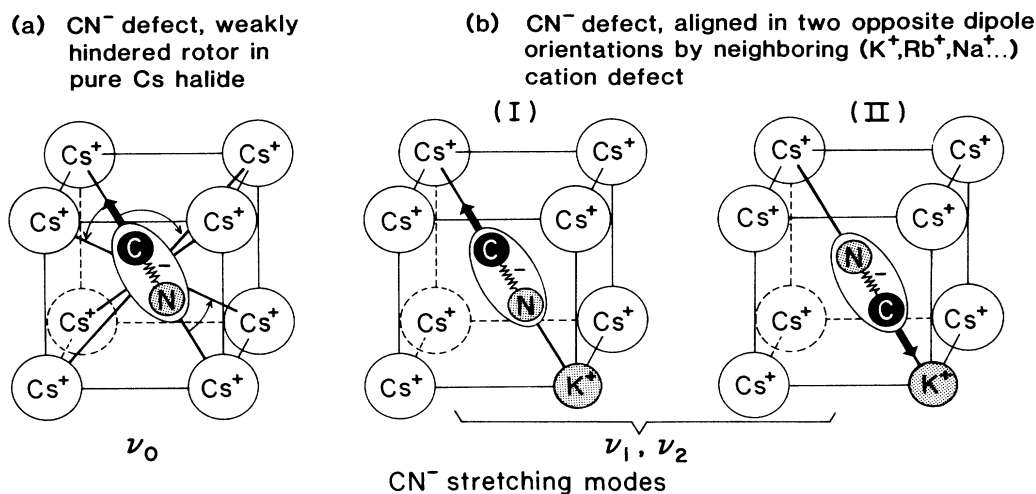


FIG. 4. Schematic illustration of microscopic structure of CN⁻ defects in cesium halides giving rise to the three observed vibrational modes. (a) Isolated CN⁻ defect: weakly hindered rotor between eight equivalent $\langle 111 \rangle$ orientations (ν_0). (b) CN⁻ defect, aligned in two opposite $\langle 111 \rangle$ electric dipole orientations by a neighboring alkali-metal-ion impurity (ν_1, ν_2).

ist between them, the two localized configurations in Fig. 4(b) would no longer be the true eigenstates of the system. Instead, gerade (*g*) and ungerade (*u*) linear combinations of them would be the eigenstates, split by the connecting tunneling matrix element energy η into $\Delta E = 2\eta$. As ir active transitions between tunneling-split vibrational levels ($v=0,1,2,\dots$) occur by $g \rightarrow u$ and $u \rightarrow g$ transitions, the vibrational absorption would be split into a doublet of splitting 4η . This interesting—but in our case very unlikely—possibility is clearly excluded experimentally: As the tunneling splitting is expected to remain very similar in the $v=0,1,2,\dots$ vibrational states, the observed splitting of the first- and second-harmonic ir transitions should be essentially the same (as was observed¹² for the tunneling free CN^- defect in KCl). In our case the observed doubling of the splitting between fundamental overtone absorption excludes this tunneling model and clearly confirms the model of two oppositely directed localized eigenstates, as illustrated in Fig. 4(b). We cannot predict at this stage which of the two configurations I and II is related to the ν_1 and which to the ν_2 vibrational lines. No simple experimental or theoretical argument is available to decide, if a higher energy (ν_1) or lower energy (ν_2) stretch mode is produced when the carbon or nitrogen end of the CN^- points to the impurity cation.

The relative number of CN^- -cation-impurity defect pairs compared to the free CN^- defects can be estimated from the integrated absorption ratio $(I_1 + I_2)/I_0$ of the $\nu_1 + \nu_2$ to the ν_0 mode. For small concentrations (N) of K^+ or Rb^+ impurities—each providing eight $\langle 111 \rangle$ neighbor places for a CN^- —we expect in purely statistical distribution a defect-pair-free- CN^- ratio of about $8N$ (e.g., for 1% Rb^+ or K^+ about 8% defect pairs). The observed integrated absorption ratios $(I_1 + I_2)/I_0$ are found for Rb^+ impurities indeed close to the statistically expected values; however, they are definitely higher for K^+ impurities (by a factor 5–6 in CsCl, a factor of 2–3 in CsBr). Apparently, increasing size misfit of both CN^- and K^+ impurities compared to the replaced host ions (CN^- is too large, K^+ too small when substituted in CsCl) produces elastic interaction which leads to preferred association of CN^- and K^+ defects. As this association may occur gradually by thermal diffusion under slow cooling of the crystal after its growth, we checked for CsCl and CsBr samples (with K^+) if quick quenching from high temperatures would freeze in a lower (e.g., statistical) amount of CN^-/K^+ defect pairs. The integrated absorption ratio $(I_1 + I_2)/I_0$, however, was not found to be changed by this quenching process.

This analysis was based on the integrated absorption ratio of the fundamental transitions, which were assumed to have the same oscillator strength for free (ν_0) and associated (ν_1, ν_2) CN^- defects. It should be noted, however, that all our measured overtone spectra show a larger (about a factor of 2) integrated absorption ratio of $(I_1 + I_2)/I_0$ compared to the fundamental spectra. (The difference can be seen visually by comparison of the first- and second-harmonic spectra in Figs. 1–3.) This relative increase of the second-harmonic absorption strength can, in principle, be produced by a stronger mechanical anharmonicity term in the potential for the CN^- stretching

motion, caused by the presence of a neighboring cationic defect. Such an explanation, however, is excluded by an important second observation: The shift of the second-harmonic compared to twice the first-harmonic frequency lies in all observed ν_0 , ν_1 , and ν_2 cases in the $22\text{--}25\text{-cm}^{-1}$ range (see Table I), demonstrating very similar mechanical anharmonicity behavior of the free (ν_0) and localized (ν_1, ν_2) CN^- modes. The only way to explain the observed equality of anharmonicity shift and nonequality of strength of the overtone absorptions for free and associated CN^- defects is the following: Besides “mechanical anharmonicity,” the electric dipole moment $p(r)$ expansion into a power series around its equilibrium point r_0 may not only have a linear term (responsible for the strength of the ir fundamental) but a sizable quadratic term, contributing to the overtone absorption strength (so-called “electric anharmonicity”¹³). We must conclude that the presence of a defect on one end of the vibrating CN^- dipole produces a change in the quadratic term of the dipole expansion, giving rise to an overtone absorption increased by electric anharmonicity.

Finally, the measured absorption intensity ratio I_1/I_2 of the two modes ν_1 and ν_2 should supply information about the population ratio of the two configurations. As we assume different ground-state energies (of difference ΔE_{12}) for the two configurations, we could most simply expect from our model a Boltzmann equilibrium behavior, leading at low temperatures ($kT \ll \Delta E_{12}$) to the occupation of only the lowest energy state. In contrast to this we observe for the different crystal systems (as mentioned in the experimental part) fixed values of $I_1/I_2 > 1$ or < 1 , which are constant over an extended low-temperature range down to 8 K. Only above rather high temperatures (typically 100–200 K) does the ratio I_1/I_2 start to approximate a value of ~ 1 .

The only reasonable explanation within our model is the following: The energy difference ΔE_{12} separating the ground states of the two opposite electric dipole orientations I and II is small compared to the energy difference ΔE_r separating the ground states of the CN^- elastic dipole orientation parallel and perpendicular to the impurity cation. This latter energy ΔE_r is needed as thermal activation energy to achieve reorientation and thermal Boltzmann equilibrium between the two low-energy states I and II, parallel to the cationic defect. Therefore only at high temperatures we will have Boltzmann equilibrium between both states. Under cooling of the crystal, the reorientation rate [$\propto \exp(-\Delta E_r/kT)$] will become slow compared to the cooling rate at some temperature T_f , such that we will freeze-in to low temperatures the Boltzmann equilibrium from T_f . This frozen-in equilibrium is reflected in the I_1/I_2 ratio, observed as a constant at low temperatures. If this interpretation is right, the absorption line of higher strength (ν_2 in CsCl and CsBr, ν_1 in CsI) represents the configuration of lower ground-state energy.

We regard the results and interpretation presented in this work as the basis for several experimental consequences, critical tests, and extensions to other techniques.

(1) Accurate measurements of the temperature and cooling-rate dependence of the I_1/I_2 ratio are under way

to test the validity and to determine quantitatively the parameters (E_{12}, E_r, T_f) for our reorientation kinetics model. Dielectric loss and thermally stimulated depolarization (TSD) effects, expected to occur in the temperature range T_f of freezing-in thermal reorientation, are under preparation for experimental measurements.

(2) The efficiency, radiative lifetime, and energy transfer of CN⁻ vibrational fluorescence, excited with a tunable color-center laser in the second-harmonic absorption of the treated orientationally localized CN⁻ defects, is at present under intense study.

(3) At higher alkali-metal-impurity concentrations, CN⁻ defects should be associated not only to single but also to pairs of Rb⁺ or K⁺ ions in different configurations, thus producing more than the two treated ν_1 and ν_2 absorption lines. We observed already at higher K⁺ or Rb⁺ doping one or two small extra lines from this origin [see Figs. 1(a), 2(a), and 2(b)], which are not present at lower doping. Particularly interesting would be a CN⁻ molecule associated in the middle of a next-nearest-neighbor pair of K⁺ ions, thus forming a $\langle 111 \rangle$ directed K⁺-CN⁻-K⁺ complex. As for this case the inversion symmetry is not broken, the two oppositely oriented CN⁻ dipole states should have equal energy and allow the dis-

cussed tunneling behavior.

(4) Using a single-mode tunable color-center laser (under buildup and testing at present), we will perform optical hole-burning experiments in the second-harmonic absorption of the rotationally localized CN⁻ defects in cesium halides, treated in this work. If this spectrally selective excitation technique can induce reorientation processes between the frozen-in I and II configurations at low temperatures, persistent holes and antiholes should appear in the ν_1 and ν_2 lines, allowing a detailed study of their static and dynamic properties. The first successful hole-burning effects in the fundamental absorption of CN⁻-Na⁺ complexes in KBr have been reported recently.¹⁰

ACKNOWLEDGMENTS

This work was supported by the National Science Foundation through Grants Nos. DMR 81-05332 and 82-11857, and for one of the authors (W.v.d.O.) by the Deutsche Forschungsgemeinschaft. We thank Y. Yang for stimulating discussions, and H. Brinkmann for measuring the spectra in Fig. 2.

*Permanent address: Fachbereich Physik, Universität-GH, D-4790 Paderborn, West Germany.

¹H. U. Beyeler, Phys. Rev. B **11**, 3078 (1975).

²A. Diaz-Gongora and F. Lüty, Phys. Status Solidi B **85**, 127 (1978).

³D. Durand and F. Lüty, Phys. Status Solidi B **81**, 443 (1977).

⁴V. Narayanamurti and R. O. Pohl, Rev. Mod. Phys. **42**, 201 (1970).

⁵Y. Yang and F. Lüty, Phys. Rev. Lett. **51**, 419 (1983).

⁶K. P. Koch, Y. Yang, and F. Lüty, Phys. Rev. B **29**, 5840 (1984).

⁷W. Gellermann, Y. Yang, and F. Lüty, Opt. Commun. **57**, 196

(1986).

⁸Th. Vetter and F. Lüty (unpublished), reported in F. Lüty, Cryst. Latt. Defects Amorphous Mater. **12**, 343 (1985).

⁹F. Lüty, Bull. Am. Phys. Soc. **30**, 390 (1985).

¹⁰R. C. Spitzer, W. B. Ambrose, and A. J. Sievers, Opt. Lett. **11**, 428 (1986).

¹¹G. R. Field and W. F. Sherman, J. Chem. Phys. **47**, 2378 (1967).

¹²F. Lüty, Phys. Rev. B **10**, 3677 (1974).

¹³G. Herzberg, *Spectra of Diatomic Molecules* (Van Nostrand, New York, 1950).